REFERENCES

(1) M. Barr, *J. Am. Pharm. Assoc.*, **NS4**, 4 (1964).
(2) J. W. McGinity and J. L. Lach, *J. Pharm. Sci.*, **66**, 63 (1977).
(3) L. H. Little, "Infrared Spectra of Adsorbed Species," Academic, New York, N.Y., 1966.
(4) R. L. Ledoux and J. L. White, *J. Colloid Interface Sci.*, **21**, 127 (1966a).
(5) B. K. G. Theng, "The Chemistry of Clay-Organic Reactions," Adam Hilger, London, England, 1974, pp. 136–210.
(6) J. M. Serratosa, *Clays Clay Miner.*, **14**, 385 (1966).
(7) M. Cruz, J. L. White, and J. D. Russell, *Isr. J. Chem.*, **6**, 315 (1968).
(8) S. Yariv, J. D. Russell, and V. C. Farmer, *ibid.*, **4**, 201 (1966).
(9) G. W. Bailey and J. L. White, *Residue Rev.*, **32**, 29 (1970).
(10) M. M. Mortland, *Clay Miner.*, **6**, 143 (1966).
(11) R. L. Ledoux and J. L. White, *Proc. Int. Clay Conf., Jerusalem*, **1**, 361 (1966).
(12) J. W. McGinity and J. L. Lach, *J. Pharm. Sci.*, **65**, 896 (1976).
(13) L. A. Pinck, W. F. Holton, and F. E. Allison, *Soil Sci.*, **91**, 22 (1961).
(14) R. E. Grim, "Clay Mineralogy," 2nd ed., McGraw-Hill, St. Louis, Mo., 1968, p. 189.
(15) C. J. Serna, G. Van Scoyoc, and J. L. Alrichs, *Am. Miner.*, **62**, 784 (1977).
(16) "United States Dispensatory," 27th ed., Lippincott, Philadelphia, Pa., 1973, p. 182.
(17) K. K. Kalnin'sh and B. G. Belen'kil, *Dan SSSR*, **157**, 619 (1964).
(18) J. L. Colaizzi and P. R. Klink, *J. Pharm. Sci.*, **58**, 1184 (1969).
(19) B. K. G. Theng, "The Chemistry of Clay-Organic Reactions," Adam Hilger, London, England, 1974, p. 18.
(20) R. Green-Kelley, *Trans. Faraday Soc.*, **51**, 412 (1955).
(21) G. W. Brindley and R. W. Hoffmann, *Clays Clay Miner.*, **9**, 546 (1962).
(22) S. A. Tahoun and M. M. Mortland, *Soil Sci.*, **102**, 314 (1966).
(23) R. E. Grim, "Clay Mineralogy," 2nd ed., McGraw-Hill, St. Louis, Mo., 1968, p. 196.
(24) R. L. Parfitt and M. M. Mortland, *Soil Sci. Soc. Am. Proc.*, **32**, 355 (1968).
(25) D. E. Williamson and G. W. Everett, Jr., *J. Am. Chem. Soc.*, **97**, 9 (1975).
(26) M. M. Mortland, J. J. Fripiat, J. Chaussidon, and J. Uytterhoeven, *J. Phys. Chem.*, **67**, 248 (1963).

ACKNOWLEDGMENTS

Supported in part by The Upjohn Co. and a National Institutes of Health biomedical research support grant.

C. J. Serna acknowledges a Fellowship from the Ministerio de Education y Ciencia, Madrid, Spain.

This report is Journal Paper 6865, Purdue University Agricultural Experiment Station, West Lafayette, IN 47907.

Physical Characterization of Erythromycin: Anhydrate, Monohydrate, and Dihydrate Crystalline Solids

P. V. ALLEN, P. D. RAHN, A. C. SARAPU, and A. J. VANDERWIELEN ˣ

Received July 5, 1977, from *The Upjohn Company, Kalamazoo, MI 49001.* Accepted for publication November 16, 1977.

Abstract □ Hot-stage microscopy, thermoanalytical methods, and X-ray powder diffraction were used to demonstrate that crystalline erythromycin dihydrate converts to the crystalline anhydrate *via* a noncrystalline intermediate. X-ray powder diffraction, IR spectral, thermogravimetric, and differential thermal analyses were used to characterize the monohydrate material. The flow interrupt technique, a procedure recently developed to deal with low surface area samples, was employed successfully in obtaining isotherms and specific surface areas for the monohydrate and anhydrate. The relative dissolution rates of the various hydrates were determined in an aqueous solution (0.01 *M* phosphate buffer, pH 7.5) at 37°. The results showed a significant difference in the dissolution rate of the dihydrate compared to the monohydrate and anhydrate.

Keyphrases □ Erythromycin—physical characterization of anhydrate, monohydrate, and dihydrate crystalline solids, dissolution rates in aqueous solution □ Hydrated forms—of erythromycin crystalline solids, physical characterization, dissolution rates in aqueous solution □ Dissolution rates—erythromycin anhydrate, monohydrate, and dihydrate crystalline solids in aqueous solution □ Antibacterials—erythromycin, physical characterization of anhydrate, monohydrate, and dihydrate crystalline solids, dissolution rates in aqueous solution

Erythromycin is a potent antibiotic effective against various microorganisms. Commercial erythromycin is a mixture of several active components. Erythromycin A (I), the major component, is unstable in acidic media. To prevent deactivation of the drug by gastric acid and to facilitate absorption in the small intestine, erythromycin can be administered as enteric-coated tablets, which are stable in acid media but dissolve in intestinal fluids. Once the enteric coating has dissolved, the absorption and therapeutic efficacy of this material may be affected by the physical characteristics of the remaining solid. It has been postulated (1) and demonstrated (2–6) that the bioavailability of various drugs can be influenced by their dissolution rate, particle size, solubility, wettability, and extent of hydration.

Erythromycin exists in many different forms, including at least two hydrates (7, 8) and an anhydrate (7), which can

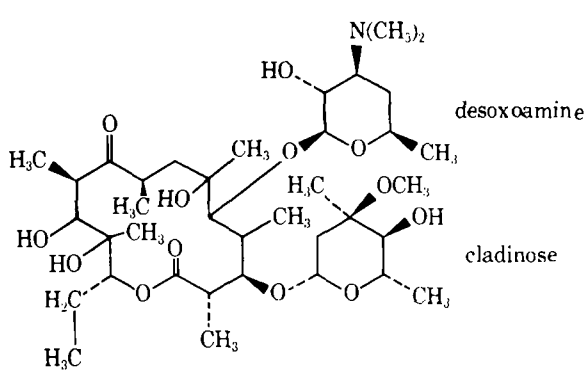

I

be differentiated by their X-ray powder diffraction patterns. The present study deals with the effects of hydration and specific surface area on the dissolution rate of erythromycin bulk drug (commercial mixture). Recent literature (9–12) indicates that the thermal behavior of crystalline drugs is not well understood. Consequently, a study of erythromycin's several hydrates was conducted to examine their thermal behavior. Special emphasis was placed on determining melting points and interconversions of the dihydrate, monohydrate, and anhydrate crystalline solids.

EXPERIMENTAL

Materials—The monohydrate and dihydrate were commercially available. The anhydrate was made from the dihydrate by drying 50 g of powdered drug for 1 week at 105° in a vacuum oven. The pressure in the oven was maintained at 5 torr or less. Nitrogen[1] and helium[1] were used in the surface area studies. Commercially available trisodium phosphate, sodium hydroxide, and erythromycin USP grade were used for the dissolution studies. Ammonium nitrate standard was used to calibrate the differential thermal analyzer.

Surface Area Measurements—All measurements were made using a dynamic flow gas adsorption system (13). For the adsorption isotherms, the desired partial pressures, P/P_0, were obtained by using premixed gases (10, 20, and 30% N_2 in helium) where convenient and by manually mixing nitrogen and helium (using the flow controls on the instrument) to obtain the other concentrations. Calibrations were effected using precision sampling gas syringes.

Samples were degassed at 60° for 30 min with a nitrogen flow of 50 ml/min. The adsorption isotherm for the dihydrate was constructed using the continuous flow method. Adsorption isotherms and surface area measurements for the monohydrate and anhydrate were performed using an interrupted flow method (14) to avoid thermal diffusion effects. All surface area values were obtained using a three-point Brunauer, Emmett, and Teller (BET) method (13).

Dissolution Apparatus—The stationary basket rotating paddle (operated at 150 rpm) consisted of the USP rotating paddle apparatus with a 12-mesh basket (Fig. 1). The basket was placed midway between the center and side of the flask, 6.5 cm from the bottom. The basket was similar in dimension to that employed in the USP rotating basket apparatus.

The metal strip at the top of the basket was tapped and screwed onto the basket lid, which was connected to a metal shaft 10 mm in diameter and 15 cm long. The metal shaft was attached to a rabbeted Plexiglas disk by a compression fitting.

The Plexiglas cover for the apparatus was countersunk around the edges so that it rested securely on the 1-liter round-bottom flask. The cover had a hole 2.54 cm in diameter in its center for the shaft of the paddle and two holes 16 mm in diameter for sampling. Another hole 2.54 cm in diameter was countersunk so that the Plexiglas disk fit flush with the cover. This fit allowed the basket to be reproducibly positioned in the flask[2].

Nine hundred milliliters of 0.01 *M* phosphate buffer (pH 7.5) at 37° was used as the dissolution medium.

Dissolution Procedure—Erythromycin bulk drug, 200 ± 6 mg, was packed into a clear gelatin capsule, size 0. Timing of the dissolution run began when the 12-mesh basket containing the capsule was immersed in the dissolution medium with the paddle rotating at 150 rpm. Aliquots of 15 ml were withdrawn with a glass syringe from the flasks at 10, 20, 30, and 60 min and replaced with 15 ml of buffer solution. The samples were immediately filtered through a 0.6-μm filter[3] into a 50-ml centrifuge tube.

The amount of erythromycin in each sample was determined by a procedure similar to the one discussed by Kuzel *et al.* (15). The procedure involves base hydrolysis [using 0.25 *M* NaOH containing 15% (w/w) Na_3PO_4] of the erythromycin by heating the mixture of base solution (2 ml) and sample (10 ml, *qs* to 20 ml) for 15 min at 60°. The absorbance (λ 236 nm) of the cooled sample was determined[4] and compared to the absorbance of a reference solution treated similarly.

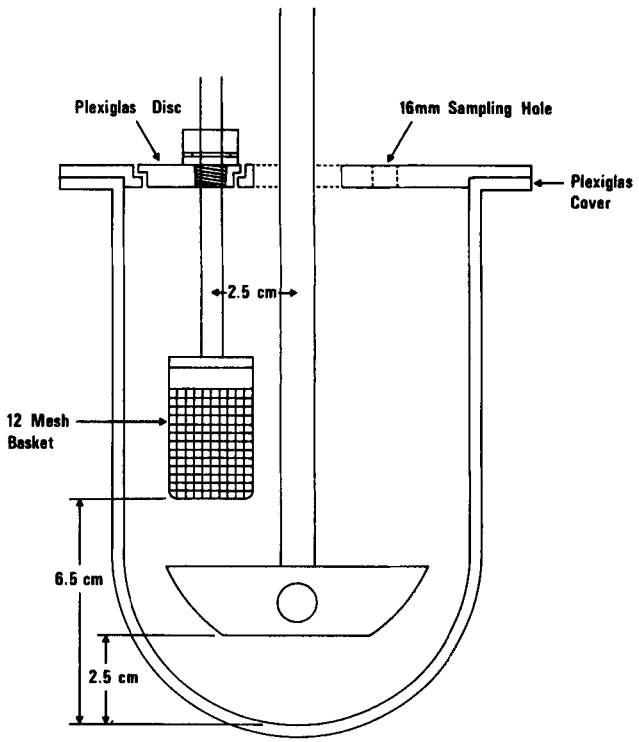

Figure 1—*Stationary basket rotating paddle dissolution apparatus.*

Thermal Analyses—The thermal behavior of erythromycin was examined using a thermal analysis system[5]. The differential thermal analysis (DTA) curves were obtained by using a standard DTA cell with a quick cool assembly. Sample tubes of 2 mm were used for the drug samples and the reference material (glass beads in all cases except one). Samples of ammonium nitrate were used to calibrate the instrument, and dry nitrogen at 50 ml/min was used to flush the DTA cell. Heating rates of 10 and 2°/min were used.

Thermal gravimetric analysis (TGA) were performed on the TGA accessory. A platinum sample pan was cleaned by heating with a Bunsen burner after each experiment. Samples (30–60 mg) were heated at 10°/min in a dry nitrogen atmosphere (flow rate = 50–60 ml/min).

The thermal stability of erythromycin was examined in both air and silicon oil, using a microscope at 125× magnification and a hot stage. Heating rates of 1–3°/min were used, and photomicrographs were taken at 20° intervals and at any significant transition points.

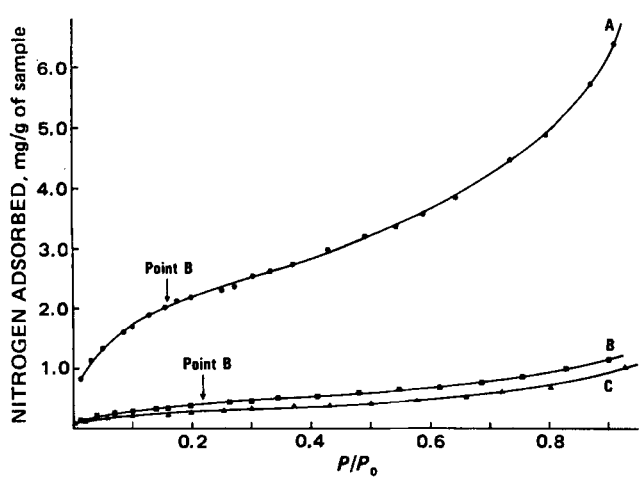

Figure 2—*Adsorption isotherms. Key: A, erythromycin dihydrate; B, erythromycin monohydrate; and C, erythromycin anhydrate.*

[1] Linde Division, Union Carbide Corp.

[2] The basket, lid, and metal shaft may be purchased from Coffman Industries. The basket and paddle were mounted on a Hansen research dissolution apparatus (model 72B-115).

[3] Millipore.

[4] Cary 11 spectrophotometer.

[5] DuPont 990 system including the 951 thermal gravimetric analysis accessory.

Table I—Comparison of Methods for Specific Area Determination on the Same Sample of Erythromycin Dihydrate

Parameter	Nitrogen Adsorption Continuous Flow	Nitrogen Adsorption Interrupted Flow	Krypton Adsorption Continuous Flow
Sample size, g	0.7028	0.0902	0.0902
Measured surface area, m^2	3.68	0.44	0.42
Specific surface area, m^2/g	5.2	4.9	4.7
Correlation coefficient	0.999	0.997	0.999

Table II—Isotherm Data for Erythromycin

Parameter	Dihydrate[a]	Monohydrate	Anhydrate
Specific surface area, m^2/g	6.6 (2.1)	1.3	1.0
Net heat of adsorption, kcal/mole at 298°K	2.4 (2.2)	1.8 ± 0.2	1.7
BET constant	55.0 (41.9)	19.6	17.3
Point B: Predicted	0.19	0.23	0.24
Actual	0.17	0.21	0.23

[a] Values in parentheses are averages of three dihydrate samples with a low measured surface area.

X-ray powder patterns were obtained using a diffractometer and powdered samples. Melt solvate analyses were performed by heating the erythromycin in an evacuated tube attached to a standard 10-cm IR gas cell. Calcium carbide was used as the drying material for the evolved gas, and an IR grating spectrometer was used to record the absorption spectra. A Fourier transform IR spectrometer also was used to identify the various hydrates.

RESULTS AND DISCUSSION

Surface Area—The adsorption isotherms for the erythromycin hydrates were all Type II (Fig. 2) (13), and their BET plots (Fig. 3) all contained linear regions of sufficient breadth to allow surface area determinations using P/P_0 values between 0.1 and 0.3. Samples of the dihydrate were analyzed by the normal continuous flow method with nitrogen as the adsorbate gas (13). This technique also was tried on the monohydrate and anhydrate but was unsuccessful because of thermal diffusion. The flow interrupt technique (14) and continuous flow with krypton as the adsorbate were examined as possible alternatives (Table I). The values obtained were comparable; however, the value obtained by krypton adsorption was slightly lower than expected. In addition, krypton adsorption was very time consuming, rarely requiring less than 10 min and occasionally longer than 2 hr for the higher P/P_0 values required in isotherms. Krypton adsorption peaks showed extensive tailing, making it difficult to determine when adsorption was complete. Therefore, the flow interrupt method was used to determine the surface area of the monohydrate and anhydrate. Adsorption was rapid, and the attainment of an equilibrium was unambiguous at all P/P_0 values since the same procedure was used as for conventional nitrogen adsorption.

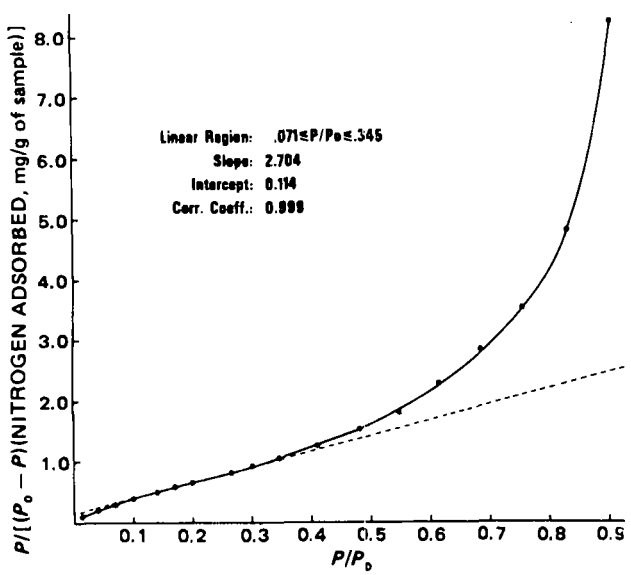

Figure 3—*Typical BET plot.*

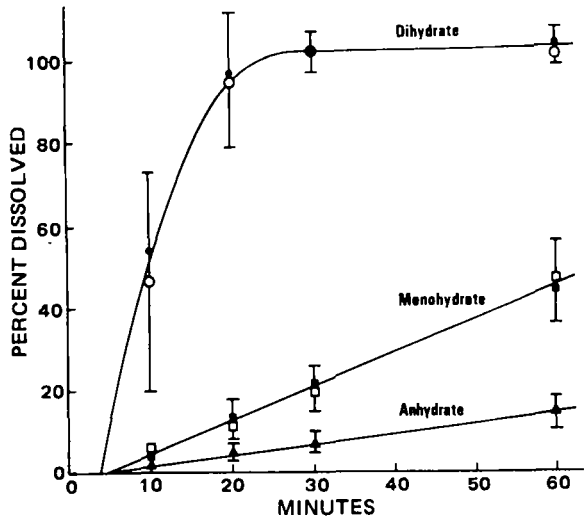

Figure 4—*Dissolution behavior of erythromycin dihydrate, monohydrate, and anhydrate in phosphate buffer (pH 7.5) at 37°. Key: ●, Sample 1; ○, Sample 2; ■, Sample 3; □, Sample 4; and ▲, Sample 5.*

The slope, S, and the extrapolated intercept, I, of the linear portion of the BET plot can then be used to calculate the weight of gas necessary to form a monolayer according to:

$$X_m = \frac{1}{S + I} \quad \text{(Eq. 1)}$$

The net heat of adsorption, ΔH_n, for a material is calculated as follows:

$$\Delta H_n = RT \ln C \quad \text{(Eq. 2)}$$

where C is the BET constant as determined from the BET plot relationship:

$$C = S/I + 1 \quad \text{(Eq. 3)}$$

However, Eqs. 2 and 3 are valid only for systems that are well defined by the BET equation (13). For such systems, the BET constant, C, may be used to predict the location of "point B" (13) (Fig. 2). This point, the beginning of the linear portion of the adsorption isotherm, was believed by Emmett and Brunauer (16) to coincide with the completion of a monolayer of adsorbate gas. A comparison of the predicted and actual point B values (Table II) indicates that the surfaces of all three hydrates are well defined by the BET equation.

The ΔH_n values for the various crystal forms were not significantly different. The small differences observed were most likely due to the amount of surface available, since the ΔH_n values and the BET constant decrease with decreasing specific surface areas.

Dissolution Studies—The results of the dissolution studies of five samples of erythromycin are depicted in Fig. 4. The dissolution curves show that the dissolution rates of the three hydrates differed significantly. The dihydrate was the fastest dissolving material while the anhydrate was less than 20% dissolved after 1 hr. Several physical parameters of the various hydrates, including surface area, net heat of adsorption (ΔH_n), and capsule packing, were examined to determine the reason for the difference in their dissolution behavior.

The results in Table III and Fig. 4 indicate that the surface area did not significantly affect the dissolution rate of erythromycin. For example, there was no difference in the dissolution rate of the two dihydrate samples, even though there was about a 2.5-fold difference in their surface

Table III—Dissolution Rate *versus* Surface Area

Sample	Percent Dissolved 20 min	Percent Dissolved 60 min	Specific Surface Area, m^2/g
1 Dihydrate	97	103	2.2
2 Dihydrate	96	101	5.2
3 Monohydrate	13	45	1.5
4 Monohydrate	11	46	1.2
5 Anhydrate	5	14	1.0

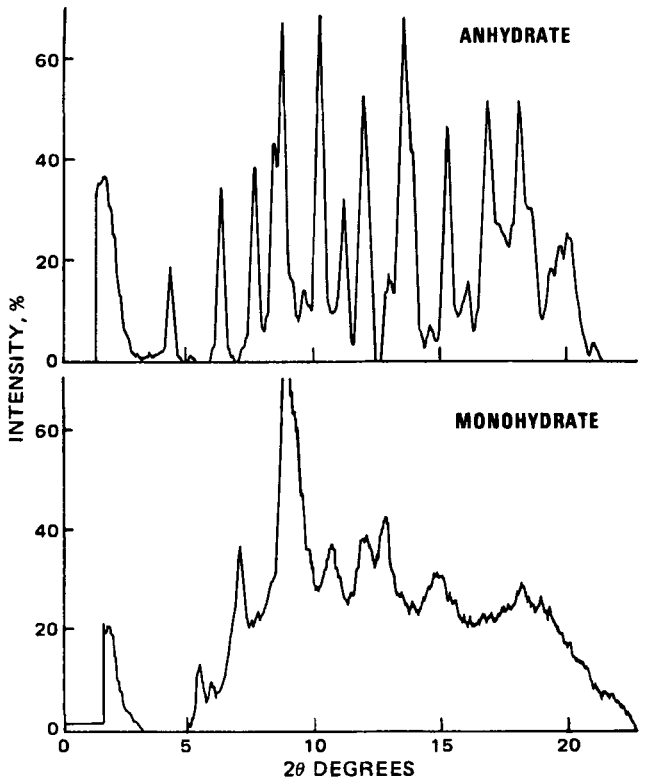

Figure 5—*X-ray powder diffraction pattern of erythromycin anhydrate and monohydrate.*

areas. As mentioned previously, there appeared to be no significant difference in the ΔH_n values of adsorption, and the difference in dissolution rates may be related to particle–particle interactions and/or the wettability of the various crystalline materials.

When performing the dissolution test on the bulk drug samples, the monohydrate and the anhydrate did not disintegrate after the gelatin capsule had dissolved, while both samples of dihydrate dispersed readily throughout the solution immediately after the gelatin capsule dissolved. To determine the effect of capsule packing on the dissolution rate of the bulk drug, 250 mg of several samples was packed into a size 1 capsule (tightly packed) and into a size 0 capsule (capsule full, packed lightly) and compared with the samples run with 200 mg of drug packed into a size 0 capsule (capsule three-fourths full and not packed) (Table IV). An examination of the percent dissolved at 20 and 60 min indicates that there was no significant difference in the dissolution rates for the various drug packings.

Shefter and Higuchi (17) found that the dissolution rate for the hydrate decreased with increasing hydration, as predicted by theory. The experimental design of the present dissolution study approximates the dosage form in which erythromycin is delivered to the small intestine. The sample is not uniformly dispersed in the dissolution medium at the start of the test. Therefore, in the present study, the dissolution rate can be affected not only by the extent of hydration but also by wettability, particle–particle interactions, and surface area.

Table IV—Packing Effects

Sample	Capsule Size[a]	Percent Dissolved 20 min	Percent Dissolved 60 min
Dihydrate	0	87	102
	1	85	101
	0[b]	96	101
Monohydrate (3)	0	9	51
	1	11	43
	0[b]	13	45
Anhydrate	1	10	19
	0[b]	5	14
Monohydrate (4)	0	7	33
	1	13	46
	0[b]	11	46

[a] Samples (250 mg) were tightly packed in the size 1 capsule and loosely packed in the size 0 capsule. [b] Two hundred milligrams of erythromycin in size 0 capsule.

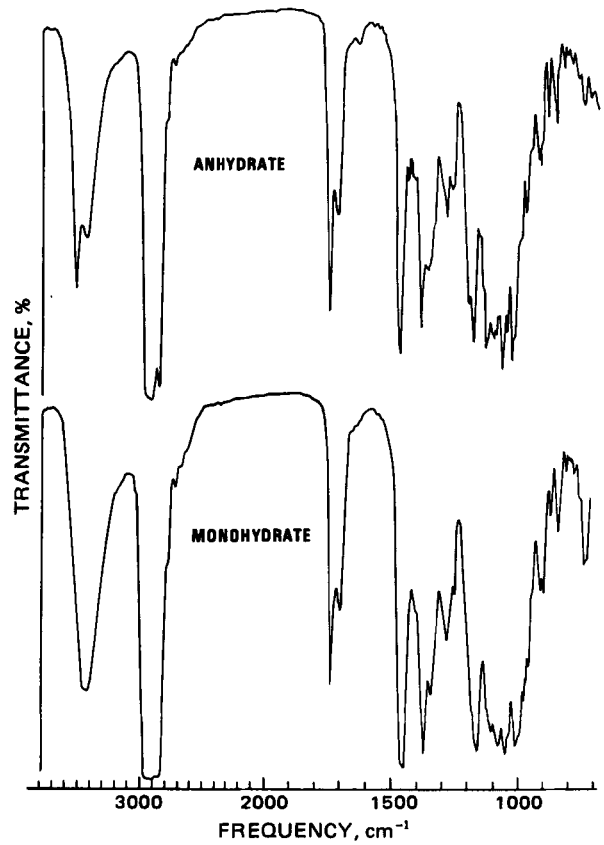

Figure 6—*IR spectrum of erythromycin anhydrate and monohydrate (mineral oil mull preparation).*

The results of Shefter and Higuchi (17) indicate that the dissolution rate of erythromycin is not determined by the extent of hydration under the present conditions. The fact that the monohydrate and the anhydrate did not disintegrate after dissolution of the gelatin capsule is further evidence that the dissolution rates of the various hydrates of erythromycin are most likely related to particle–particle interactions and wettability.

Phase Transitions—The identities of the anhydrate and dihydrate crystalline materials were verified by comparing their X-ray powder diffraction patterns to known references (7). The monohydrate was characterized by its X-ray powder diffraction pattern (Fig. 5), IR spectrum (Fig. 6), and the fact that it contained a stoichiometric amount of water (Table V). The observed weight loss was 2.6% as compared to a

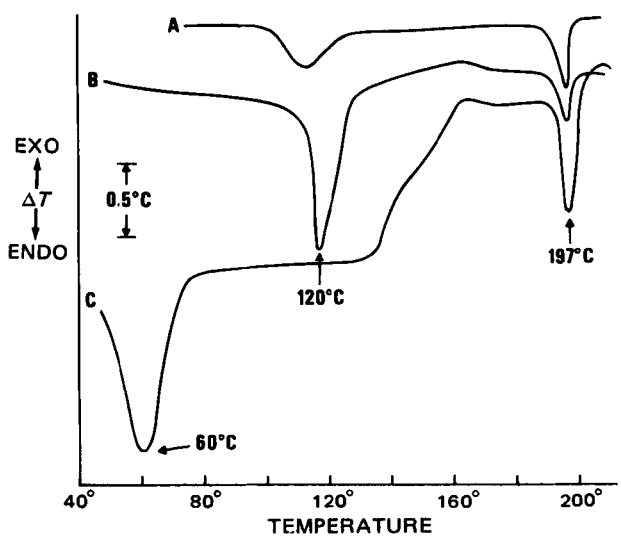

Figure 7—*DTA curves for the erythromycin dihydrate. Key: A, oil mull, nitrogen flow; B, powder sample, nitrogen flow; and C, powder sample, air pressure at 1 torr or less. Heating rate was 10°/min.*

Table V—Thermogravimetric Analysis

Erythromycin		Experimental Temperature Range	Weight Loss, % of Sample
Before Heating	After Heating		
Dihydrate	Dihydrate and amorphous	25–135°	4.6 (average of 6)
	Amorphous	25–135°, 135° for 10 min	4.7
	Anhydrate and amorphous	25–172°	4.6
Monohydrate	Amorphous	25–140°	2.6 (average of 2)
	Amorphous	25–140°, 140° for 10 min	—
	Anhydrate and amorphous	25–180°	2.5
Anhydrate	Anhydrate	25–150°	0.8 ± 0.3

Table VI—Hot-Stage Microscopy Results

Starting Material	Dehydration Temperature Range	Phase Transition to Amorphous	Recrystallization to Anhydrate	Anhydrate Melting
		Air Mount[a]		
Dihydrate	Not observed	129–132°	136–185°	189–192°
Monohydrate	Not observed	124–130°	Not observed	Not observed
Anhydrate	Not observed	Not observed	Not observed	190–193°
		Oil Mount[b]		
Dihydrate	95–130°	Not observed	100–125°	190–195°
Monohydrate	Not observed	114–137°	119–190°	190°
Anhydrate	Not observed	Not observed	Not observed	190–193°

[a] Crystals were exposed to the atmosphere. [b] Crystals were suspended in silicon oil.

theoretical value of 2.4%. Pelizza *et al.* (11) indicated that the monohydrate described previously (8) was the anhydrate containing surface moisture. The present TGA, IR, and X-ray data indicate that the monohydrate is a crystalline material containing one molecule of hydrated water for each molecule of erythromycin. However, the X-ray data (Fig. 5) indicate that the monohydrate does not possess the same degree of crystallinity as the anhydrate.

The results shown in Fig. 7 and Table V demonstrate that erythromycin dihydrate converts to the anhydrate *via* a noncrystalline intermediate when it is heated from 25 to 220° in a dry nitrogen atmosphere as shown by the reactions in Scheme I:

$$A\cdot 2H_2O_{(CS)} \xrightarrow[\text{dehydration}]{\sim 120^\circ} A_{(CS)} + 2H_2O_{(g)}$$

$$A_{(CS)} \xrightarrow{120\text{–}135^\circ} A_{(a)}$$

$$A_{(a)} \xrightarrow{120\text{–}190^\circ} A^{*}_{(CS)}$$

$$A^{*}_{(CS)} \xrightarrow[\text{melting}]{190\text{–}193^\circ} A_{(l)}$$

Scheme I

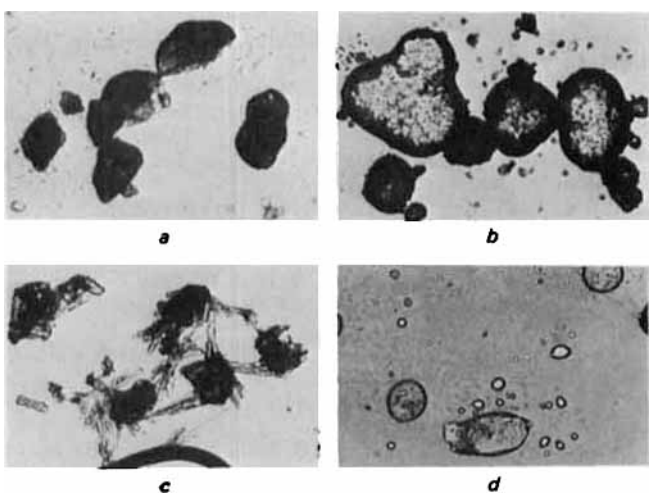

Figure 8—*Photomicrographs of the erythromycin dihydrate taken during the hot-stage microscopy study. Key:* a, *25°, crystalline solid, suspended in oil;* b, *140°, amorphous material, exposed to atmosphere;* c, *180°, crystalline solid, suspended in oil; and* d, *193°, isotropic liquid, suspended in oil.*

where A is erythromycin, a is amorphous, CS is crystalline solid, and l is isotropic liquid. $A^{*}_{(CS)}$ was determined to be the anhydrate crystal form by X-ray diffraction and DTA. The amorphous material was identified by X-ray powder diffraction. The diffraction pattern of amorphous and noncrystalline solids consists of very diffuse reflections since there are no parallel planes of atoms as are normally found in crystalline materials (17). The term amorphous, strictly speaking, means a completely random orientation, which is rarely the case in solid materials. The present study did not establish if the noncrystalline (amorphous) intermediate could be strictly classified as amorphous. However, the material had a glossy appearance, and no reflection planes were observed by X-ray powder diffractometry.

Verification of the dehydration endotherm observed at approximately 120° can be made by the following observations: (*a*) the weight loss (average = 4.65%) is equivalent to the stoichiometric loss of two water molecules, (*b*) a melt solvent analysis shows that the gas evolved is water, and (*c*) the dehydration endotherm (Fig. 7) is pressure dependent, as expected for a reaction involving a volume change.

A careful examination of erythromycin hydrates (Table V) by X-ray powder diffraction showed that the material produced at approximately 135° was amorphous and that the melting reported previously (8, 11, 18, 19) was the formation of a fluid noncrystalline solid and not the formation of an isotropic liquid.

A hot-stage microscopy study was conducted to gain further insight into the thermal behavior of erythromycin. The results (Table VI and Fig. 8) confirm the X-ray, TGA, and DTA findings. The medium used to suspend the erythromycin crystals on the microscope slide had a very pronounced effect on its thermal behavior. The data in Table VI show that when the crystals were left open to the atmosphere, one observed the transition of the dihydrate to an amorphous state and then recrystallization to the anhydrate form. However, when the crystals were covered with silicon oil, the formation of the amorphous state was apparently too rapid to observe (Table VI) since only the formation of the anhydrate was seen. When a DTA of erythromycin dihydrate (Fig. 7, curve A) was performed under similar conditions, the exotherm normally observed between 120 and 190° was not present. The dehydration endotherm was shallow and broad, indicating that recrystallization was probably occurring simultaneously with dehydration.

Table VII—DTA Results: Slow Heating [a]

Starting Material	Dehydration Endotherm[b]	Phase Change Exotherm	Melting Endotherm[b]
Dihydrate	120°	130–185°	192°
Monohydrate	111°	Not observed	185°
Anhydrate	None	None	191°

[a] Heating rate = 2°/min; atmosphere = nitrogen flow. [b] Values reported here are the peak temperatures of the endotherms.

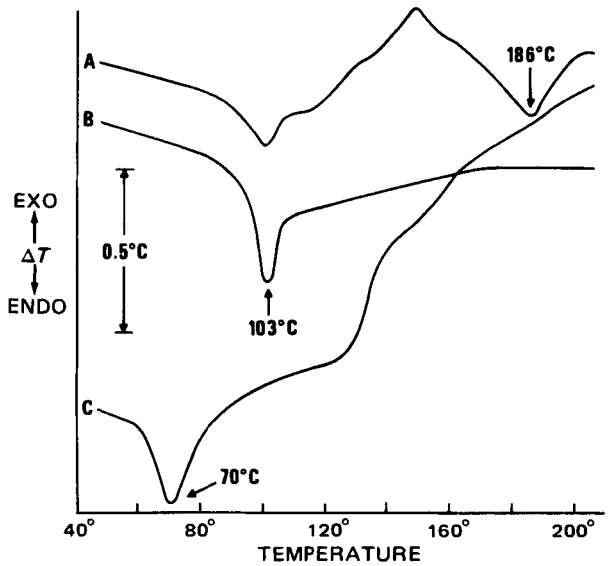

Figure 9—*DTA curves for the erythromycin monohydrate. Key: A, oil mull, nitrogen flow; B, powder sample, nitrogen flow; and C, powder sample, air pressure at 1 torr or less. Heating rate was 10°/min.*

The DTA and hot-stage microscopy studies also were performed on the monohydrate (Figs. 9 and 10). The thermal behavior of the monohydrate in the presence of silicon oil or at slow heating rates (Table VII) is described by the following reactions:

$$A\cdot H_2O \xrightarrow[\text{dehydration}]{\sim 100^\circ} A_{(CS)} + H_2O_{(g)}$$

$$A_{(CS)} \xrightarrow{114\text{–}137^\circ} A_{(a)}$$

$$A_{(a)} \xrightarrow{120\text{–}190^\circ} A^*_{(CS)}$$

$$A^*_{(CS)} \xrightarrow[\text{melting}]{186\text{–}190^\circ} A_{(l)}$$

Scheme II

The main difference observed during the thermal analyses of the monohydrate material was the rate at which the recrystallization occurred. The formation of crystalline material from the amorphous fluid was observed only in oil media (Fig. 10) and during very slow heating on the DTA apparatus (Table VII). Crystalline material did not form in sufficient quantity during the TGA experiments to confirm the presence of the anhydrate. However, the hot-stage microscopy and DTA melting-point data (Tables VI and VII) indicate that the crystalline erythromycin anhydrate was formed.

Hot-stage microscopy and DTA results (Tables VI and VII) for the anhydrate suggest that it is a monotropic crystal form, since the only transition observed was melting (190–193°) to the isotropic liquid of erythromycin. The thermogravimetric results (Table V) indicate that only surface moisture was present, which is further verified by the fact that no dehydration endotherms were observed during the DTA experiments.

SUMMARY AND CONCLUSIONS

Examination of the several physical properties of the dihydrate, monohydrate, and anhydrate indicates that their dissolution rates are probably related to particle–particle interactions and/or wettability of the various hydrates. The anhydrate had the slowest dissolution rate while the dihydrate dissolved very quickly in comparison to the monohydrate and anhydrate. No correlation was observed between the dissolution rate and specific surface area of the drug.

There has been a great deal of confusion concerning the melting point of crystalline solids (8, 9, 11, 12). The present study on erythromycin indicates that the dihydrate and monohydrate convert to the anhydrate (mp 190–193°) *via* an amorphous intermediate. The dihydrate appears

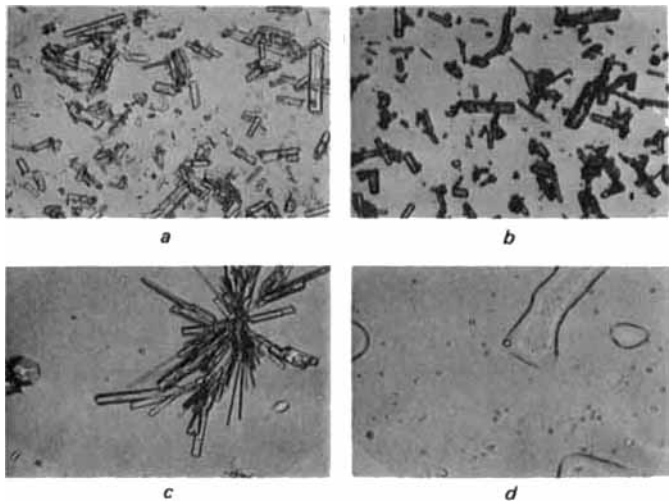

Figure 10—*Photomicrographs of the erythromycin monohydrate taken during the hot-stage microscopy study. Key:* a, *25°, crystalline solid, suspended in oil;* b, *122°, amorphous material, exposed to atmosphere;* c, *180°, crystalline solid, suspended in oil; and* d, *189°, isotropic liquid, suspended in oil.*

to convert readily when it is heated, but the monohydrate converts to the anhydrate only in the presence of silicon oil or if it is heated very slowly. When erythromycin monohydrate was heated at 10°/min, only the formation of the amorphous material was observed. Since the amorphous phase can be described as a fluid whose viscosity varies with temperature (*e.g.*, glass has a viscosity high enough to resemble a solid at ambient temperatures), the phase change from a crystalline solid to a noncrystalline material can be described as a melting point. But if the strict definition of melting is adhered to (*i.e.*, that melting involves the formation of an isotropic liquid), then the melting point observed at 190–193° was the only true melting point observed for the erythromycin forms examined. The change from the amorphous phase to the isotropic liquid involves very low transition energies and, therefore, is very difficult to observe.

It is obvious from this discussion that one must be very careful when assigning the melting point of a crystalline solid. This study shows that the melting point at 130–135° reported for erythromycin dihydrate (19) and monohydrate (8) is the formation of the amorphous phase and not a true melting point. It appears that the anhydrate crystal form is the most stable and that its melting point at 190–193° is the true melting point of crystalline erythromycin base.

REFERENCES

(1) J. T. Carstensen, "Theory of Pharmaceutical Systems," vol. II, Academic, New York, N.Y., 1973, p. 262.

(2) J. H. Fincher, *J. Pharm. Sci.*, **57**, 1825 (1968).

(3) A. J. Aguiar, J. Krc, Jr., A. W. Kinkel, and J. C. Samyn, *ibid.*, **56**, 847 (1967).

(4) A. J. Aguiar, L. M. Wheeler, S. Fusari, and J. E. Zelmer, *ibid.*, **57**, 1844 (1968).

(5) A. J. Aguiar and J. E. Zelmer, *ibid.*, **58**, 983 (1969).

(6) J. W. Poole, G. Owen, J. Silverio, J. N. Feyhof, and S. B. Roseman, *Curr. Ther. Res.*, **10**, 292 (1968).

(7) Eli Lilly Co., U.S. pat. 2,864,817 (Dec. 16, 1958).

(8) M. G. Shtolts, L. K. Shtamm, N. P. Bednyagina, and A. K. Shtolts, *Antibiotiki*, **11**, 291 (1966).

(9) M. A. Moustafa, A. R. Ebian, S. A. Khalil, and M. M. Motawi, *J. Pharm. Pharmacol.*, **23**, 868 (1971).

(10) J. Matsunagan, N. Nambu, and T. Nagai, *Chem. Pharm. Bull.*, **24**, 1169 (1976).

(11) G. Pelizza, M. Nebuloni, and G. G. Gallo, *Farmaco, Ed. Sci.*, **31**, 254 (1976).

(12) J. Haleblian and W. McCrone, *J. Pharm. Sci.*, **58**, 911 (1969).

(13) S. J. Gregg and K. S. W. Sing, "Adsorption Surface Area and Porosity," Academic, New York, N.Y., 1967.

(14) B. G. Tucker, *Anal. Chem.*, **47**, 778 (1975).

(15) N. R. Kuzel, J. M. Woodside, J. P. Caner, and E. E. Kennedy,

Chemotherapy, **4**, 1234 (1954).
(16) P. H. Emmett and S. Brunauer, *J. Am. Chem. Soc.*, **59**, 1553 (1937).
(17) E. Shefter and T. Higuchi, *J. Pharm. Sci.*, **52**, 781 (1963).
(18) J. K. Haleblian, *ibid.*, **64**, 1269 (1975).
(19) E. H. Flynn, M. V. Signal, P. F. Wiley, and K. Gerzon, *J. Am. Chem. Soc.*, **76**, 3121 (1954).

ACKNOWLEDGMENTS

The authors thank D. S. Aldrich for the excellent photomicrographs and K. G. Zipple for obtaining the X-ray diffraction patterns that were used for crystal form identification. They also acknowledge the assistance of C. E. Stiller (surface area determinations) and C. W. Andrews (DTA and TGA analyses of the monohydrate crystal forms).

GLC Determination of Caffeine in Plasma Using Alkali Flame Detection

JORDAN L. COHEN *ˣ, CHI CHENG *, JAMES P. HENRY ‡, and YUEN-LING CHAN *

Received August 15, 1977, from the **School of Pharmacy and the* ‡*School of Medicine, University of Southern California, Los Angeles, CA 90033.* Accepted for publication November 29, 1977.

Abstract □ A rapid, specific, and sensitive GLC assay for caffeine in plasma was developed utilizing alkali flame-ionization detection. The procedure involves the addition of mepivacaine as an internal standard, alkalinization of the sample, and extraction with chloroform. Peak height ratio measurements produced linear standard curves in the 0.25–10.0-μg/ml range. Absolute sensitivity from a 1.0-ml plasma sample was 0.1 μg/ml. The relative standard deviation of a 2.0-μg/ml pooled plasma standard run repeatedly over several months was 5.2%. The method is applicable to time–concentration studies in human and animal plasma following typical oral doses of caffeine.

Keyphrases □ Caffeine—GLC analysis in plasma □ GLC—analysis, caffeine in plasma □ Stimulants, central—caffeine, GLC analysis in plasma

The widespread occurrence of caffeine in popular beverages and over-the-counter medications makes it the drug most consumed by many individuals. The average amount of caffeine in a cup of coffee is about 80–100 mg; however, depending on the manner of preparation, strong coffee can contain as much as 300 mg/cup (1). The amount of caffeine in tea varies considerably, mainly as a function of water temperature and time of contact, with typical averages of 25–50 mg/cup (1). However, caffeine concentrations in tea approach those of coffee when packaged instructions for typical products are followed. Cola and cocoa beverages contain smaller, but substantial, amounts of caffeine.

BACKGROUND

Although caffeine has long been known for its diuretic and central nervous system stimulating activities, many other pharmacological and some toxic effects have been reported, particularly in individuals consuming large quantities. Gilbert (2) reviewed a large number of epidemiologic studies suggesting that ulcers of the stomach and duodenum, carcinomas of the kidney and urinary tract, and certain types of heart disease occur more frequently in individuals ingesting more than 600 mg of caffeine/day. In addition, a large number of symptoms associated with anxiety occur more frequently in this group.

These reports prompted investigations of the relationships among caffeine consumption, adverse effects, and body fluid concentrations. Rather surprisingly, there is a scarcity of published methods suitable for the routine determination of caffeine. The spectrophotometric method of Axelrod and Reichenthal (3) is widely used, as is a modified procedure (4), but these procedures have distinct sensitivity and specificity limitations and are relatively tedious. A GLC method (5) was reported with improved sensitivity, but it suffered from an inadequate internal standard which was added just prior to injection and hampered the reproducibility.

Although several liquid chromatographic methods were reported for theophylline (6, 7), none has been reported specifically for caffeine. Caffeine elutes slowly and broadly in these systems. A radioimmunoassay with a high level of sensitivity recently was reported (8). The inherent specificity of GLC, coupled with the increased sensitivity and selectivity of an alkali flame detector for nitrogen-containing compounds, led to the development of the present assay for caffeine in plasma of animals and humans. Data also are presented that support the application of this method for obtaining plasma time–concentration data on caffeine after ingestion of typical doses.

EXPERIMENTAL

Reagents—Caffeine[1] (purity >99%) was obtained commercially and used directly. A standard stock solution containing 200 μg/ml was prepared in methanol, protected from light, and stored at 4°.

Mepivacaine, the internal standard, was prepared by extraction of the alkalinized commercial dosage form[2] with dichloromethane. The solvent was removed, and the solid was recrystallized from ether, mp 150–152°. A standard stock solution containing 650 μg/ml was prepared in methanol and stored in the same manner as the caffeine stock solution.

Chloroform[3] and methanol[3] were spectral grade. All other reagents were analytical grade and were used as received. Other drugs were commercially available dosage forms.

Standard Curve—Appropriate aliquots of the stock caffeine standard in methanol were added to conical centrifuge tubes, the solvent was evaporated, and 1.0 ml of pooled human plasma was added to produce final concentrations of 0.25, 0.5, 1.0, 5.0, and 10.0 μg/ml. Identical concentrations were used to prepare aqueous standard curves. The tubes were vortexed to dissolve the drug, and the assay was carried out as described later. Standard curves were constructed from peak height ratio measurements of caffeine to internal standard.

Analytical Procedure—To 1.0 ml of plasma or aqueous sample in a 15-ml centrifuge tube were added 25 μl of mepivacaine standard in methanol and 30 μl of 12 *N* NaOH. This solution was vortexed, 10.0 ml of chloroform was added, and the tube was shaken for 15 min. The tube was then centrifuged at 2500 rpm for 10 min, and the aqueous (top) layer was aspirated off. The organic layer was filtered[4] into a 15-ml centrifuge tube and evaporated using a stream of air in a 40° water bath. The residue

[1] Aldrich Chemical Co., Milwaukee, Wis.
[2] Carbocaine Hydrochloride, Winthrop Laboratories, New York, N.Y.
[3] Burdick and Jackson Laboratories, Muskegon, Mich.
[4] Whatman No. 1 filter paper.

0022-3549/78/0800-1093$01.00/0